Available online at www.sciencedirect.com
SCIENCE DIRECT
Polymer 46 (2005) 11591–11599
polymer
www.elsevier.com/locate/polymer

Rheological study of carbon nanofiber induced physical gelation in polyolefin nanocomposite melt

Antonis Kelarakis [1], Kyunghwan Yoon, Rajesh H. Somani, Xuming Chen, Benjamin S. Hsiao *, Benjamin Chu **

Department of Chemistry, Stony Brook University, Stony Brook, NY 11794-3400, USA

Received 16 June 2005; received in revised form 29 September 2005; accepted 1 October 2005
Available online 25 October 2005

Abstract

The rheological behavior of nanocomposites based on elastomeric ethylene–propylene (EP) random copolymer (84.3 wt% P) and well-dispersed modified carbon nanofibers (MCNFs) with concentrations from 0.5 to 20 wt% were studied by oscillatory-shear rheometry at varying temperatures. At relatively low temperatures, the entanglement density of the polymer chains appeared to increase with filler concentration, ensuring strong MCNF–polymer interactions. At elevated temperatures, pronounced deviations from the ideal melt behavior in the low frequency domain (i.e. positive slopes of the tan $\delta(\omega)$ curves) were observed, indicating the formation of a three-dimensional percolated network. Following the Winter–Chambon criterion, the transition from pseudo-solid-like to liquid-like behavior (i.e. the critical gel point) upon cooling was determined. The physical gelation induced by MCNFs is a thermo-reversible phenomenon and its origin can be traced to the interactions of nanofillers, where the percolation temperature decreases with filler concentration. Abrupt changes in the critical gelation temperature, the stiffness of the gel and the relaxation exponent were observed in nanocomposites with MCNF loading above 10 wt%. This behavior indicates a change of the mechanism of physical gelation at high MCNF loadings that can be explained by the concept of bridge formation of polymer segments between two adjacent nanofillers in concentrated nanocomposites.

Keywords: Ethylene–propylene elastomer; Carbon nanofiber; Nanocomposite

1. Introduction

Carbon nanotubes (CNTs) and carbon nanofibers (CNFs) have attracted a great deal of interest in the scientific community because they combine the advantages of small diameter, extremely high aspect ratio, and graphitic surface with sp^2 carbon-hybridized structure that can be functionalized. These unique properties make this new class of carbon allotropes appealing candidates for a wide range of applications [1,2]. Nowadays, these materials can be produced on a relatively large scale in an economical way, such as by carbon-arc discharge, laser ablation of carbon and chemical vapor deposition. Incorporation of CNTs and CNFs into polymers can result in a new generation of engineering materials with high-performance properties. For example, CNT-based nanocomposites exhibited significant mechanical improvement [3–5], high electrical conductivity [6] and superior thermal properties [6].

One of the key points to the successful development of CNT-based nanocomposites is the surface functionalization of the fillers [7–10]. This is an essential step to overcome the inherent incompatibility between the nanofiller and polymer matrix, thus ensuring significant energy and load transfer across the nanofiller-matrix interface. Another issue that can be controlled by surface functionalization is to prevent the strong tendency of nanofiller aggregation. Several approaches, all involving the attachment of functional groups on the graphitic sidewalls, have been proposed [7–10]. It was found that non-covalent exo- and endo-hedral chemistry could be successfully used to enhance the nanofiller dispersion in liquid media, whereas covalent bonding could further promote the nanofillers incorporation into polymeric matrices.

In this study, the surface of CNFs has been chemically grafted with short polypropylene chains, which is also

* Corresponding authors. Tel.: +1 631 632 7793; fax: +1 631 632 6518.
** Tel.: +1 631 632 7928; fax: +1 631 632 6518.
E-mail addresses: bhsiao@notes.cc.sunysb.edu (B.S. Hsiao), bchu@notes.cc.sunysb.edu (B. Chu).
[1] Current address: Department of Materials Science and Engineering, Cornell University, Ithaca, NY 14853,USA.

0032-3861/$ - see front matter © 2005 Elsevier Ltd. All rights reserved.
doi:10.1016/j.polymer.2005.10.009

the major component of the thermoplastic ethylene–propylene (EP) random copolymer matrix. A unique elastomeric nanocomposite based on polypropylene modified carbon nanofibers (MCNFs) and EP copolymer with dominant P content was thus prepared. The rheological behavior of this nanocomposite at temperatures above the nominal melting point of the polymeric matrix ($T_m < 50$ °C) [11] was systematically investigated with a particular emphasis to gain new insights into the evolution of gelation response. The system can also be thought of as a model system for the control of processability in nanocomposite melts through physicochemical means.

Rheological methods have been widely used to monitor the gelation behavior, since they can detect the presence of internal structures [12,13]. Physical gels can be viewed as a percolated three-dimensional (3D) network, in which the macroscopic connectivity arises from physical interactions. The long-range connectivity can be attributed to various forces, such as van der Walls, hydrogen bonds and electrostatic interactions, induced by cross-linking formation due to the presence of physical aggregates, crystals or fillers. At the gel point, the viscoelastic response of the system changes from liquid-like to pseudo-solid-like behavior. Physical gelation in polymeric matrices induced by carbon black [14], carbon nanotubes [15–18] and nanoclays [19,20] has been reported. For example, it has been suggested that carbon black can aggregate into a percolated superstructure mediated by polymeric chains absorbed on the interface [14]. Similarly, exfoliated layer silicates or stacks of intercalated layered silicates in nanocomposites containing organoclays can also form a percolated network [18]. The rheological response of aqueous suspensions of single-wall CNTs has been used to model the percolation of rigidity induced by rod particles [21]. The viscoelasticity of polymer matrices filled with single- and multi-wall CNTs and CNFs has also been investigated to some extent. Although the gelation behavior in this class of nanocomposites has been well documented, it is more qualitative in nature rather than quantitatively described.

The present study is an attempt to bridge the gap of quantitative information in the literature of physical gelation in nanocomposites. We selected CNFs rather than CNTs because CNFs are easier to be functionalized due to the layer edge defects by the presence of tilted graphite layers to the CNF axis [22]. The choice of the recently commercialized EP copolymer [23] as the polymer matrix is because this material is elastomeric but can be processed as thermoplastics and possesses interesting mechanical properties [24,25]. Moreover, due to its low crystallization kinetics, this polymer remains amorphous, even at a high degree of supercooling for a long period of time (this behavior was confirmed by DSC measurements). Thus, the analysis of the rheological data is simplified, since the effects due to the presence of crystals [12] can be excluded. The chosen system thus can be viewed as a model to understand the gelation behavior in nanocomposite melt with nanofibrous fillers.

2. Experimental

2.1. Materials and preparation

The EP random copolymer sample was provided by ExxonMobil Chemical Company and it is a member of the commercial 'Vistamaxx' specialty elastomers [11]. The copolymer was synthesized with the aid of discrete metallocene catalyst. It had 84.3 wt% propylene (P) content with the number-average molecular weight $M_n = 9.6 \times 10^4$ g/mol and weight-average molecular weight $M_w = 1.7 \times 10^5$ g/mol. Carbon nanofibers (CNFs) were obtained from Applied Sciences with the trade name Pyrograf III (PR-24-HHT). The diameters of these CNFs varied from 60 to 150 nm and the estimated length was between 30,000 and 100,000 nm. The CNF sample was used without any purification.

A low-molecular weight polypropylene-*graft*-maleic anhydride polymer ($M_w = 9100$ g/mol, $M_n = 3900$ g/mol and acid number = 47 mg KOH/g) was purchased from Aldrich and was used without further treatment. This polymer was used to modify the CNF sidewalls. The chemical scheme, the procedures followed and the characterization of the received functionalized CNFs have been presented in detail elsewhere [24]. Here we briefly present the procedures as followed [25,26]. The CNFs were first oxidized in a sulfuric/nitric acid mixture (volume ratio = 3:1) at 60 °C for 2 h. The oxidized CNFs were then reduced by sodium borohydride in absolute ethanol at 80 °C for 5 h. The resulting CNFs and polypropylene-*graft*-maleic anhydride polymer were mixed in 1,2 dichlorobenzene and then heated up to 120 °C with stirring for 5 h. The suspension was filtered in hot 1,2-dichlorobenzene and washed several times with warm 1,2-dichlorobenzene. The filtered solid was put into the soxhlet extraction apparatus and refluxed for several days with cyclohexane until it reached a constant weight to ensure complete removal of the unattached polymer.

Polypropylene-grafted CNFs (we termed it MCNFs from hereon, ~0.2 g in the case of 20 wt% nanocomposite) were dispersed in xylene (440 ml) using an ultrasonicator for 30 min. EP copolymer was subsequently added to the CNF suspension at 120 °C and stirred for 2 h. The mixture was precipitated into cold methanol (~2 l), filtered, and dried at 90 °C in vacuum for a day. The same procedure was followed for the preparation of the 0.5, 1, 5 and 10 wt% nanocomposites.

2.2. Characterization techniques

The nanocomposite sample was immersed in liquid nitrogen for 3 min and then cut by a razor blade to prevent deformation of the cross-section area for microscopy examination. Scanning electron microscopic (SEM) images were obtained using a Leo 1550 microscope operated at an acceleration voltage of 10 kV. The sample was subject to gold coating to reduce the charging effects. Fig. 1 shows a typical SEM image of a 20 wt% MCNF-EP nanocomposite (the most concentrated sample investigated), taken along the cross-section of the prepared sample, at room temperature. The dispersion of

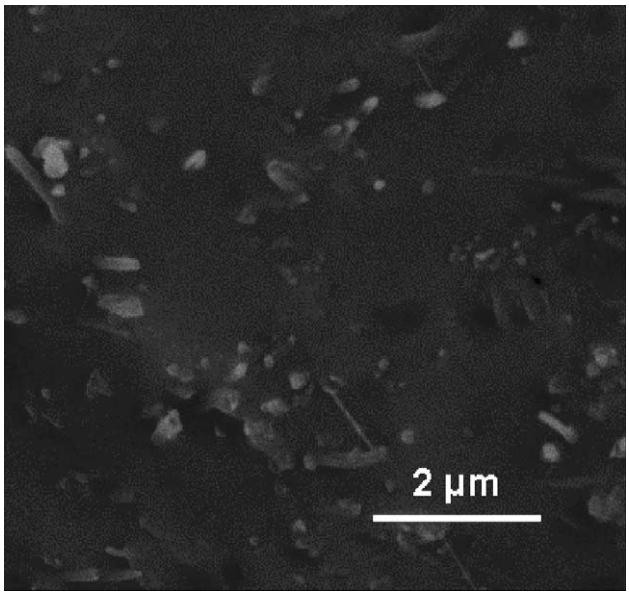

Fig. 1. SEM image of a 20 wt% MCNF-EP nanocomposite taken along the cross-section at room temperature.

MCNFs in the nanocomposite appeared homogenous without any sign of MCNF aggregation, suggesting that excellent interactions, such as van der Waals, exist between the MCNF and the polymer matrix in the prepared samples.

Dynamic rheological properties of the nanocomposite samples were determined by using a strain-controlled rheometer RMS-605 (rheometrics scientific) equipped with parallel plate geometry (diameter 25 mm). The samples were held at 220 °C for 5 min in order to erase the memory of thermal and mechanical effects and were then cooled to the experimental temperatures. The temperatures were scanned with 0.5 °C steps, with an accuracy of ±0.1 °C. A time interval of 20 min was allowed for thermal equilibrium before the measurement. Dry nitrogen was maintained to suppress the oxidative degradation at high temperatures. Storage and loss moduli were recorded in the oscillatory-shear mode, across the frequency range between 0.05 and 79 rad/sec. The strain amplitude was adjusted for each sample so that a clear signal was obtained, while remaining within the linear viscoelastic region.

2.3. Physical gelation by rheology

Gelation can be monitored by rheological methods because rheology is a sensitive tool to probe the internal structures. At the gel point, the system is known to relax in a universal, self-similar time function [27,28]:

$$G(t) = St^{-n} \tag{1}$$

where S is the stiffness of the gel and n is the relaxation exponent ($0<n<1$). The above equation can be rewritten in terms of storage G' and loss G'' moduli

$$G'(\omega) = S\Gamma(1-n)\cos\left(\frac{n\pi}{2}\right)\omega^n \tag{2}$$

$$G''(\omega) = S\Gamma(1-n)\sin\left(\frac{n\pi}{2}\right)\omega^n \tag{3}$$

where ω is the angular frequency and Γ is the gamma function. Eqs. (2) and (3) imply that at the gel point, $\tan\delta = G''/G'$ is frequency independent with

$$n = \frac{2\delta}{\pi} \tag{4}$$

Therefore, from a rheological point of view, the evolution of gel can be characterized by a zero-slope plateau in the $\tan\delta$ curve. This observation is widely known as the Winter–Chambon criterion [27,28]. Despite the fact that this criterion was originally developed to describe the chemical gelation process, it is now well accepted that it can also be applied to physical gels. In principle, the zero-slope plateau in the $\tan\delta$ curve reflects the equilibrium between two opposite factors: the slope of $\tan\delta$ curves is negative for melts, but positive for solids. It should be emphasized that the plateau in the $\tan\delta$ curve is observed in the low frequency regime rather than the entire spectrum. Therefore, access to the low frequency data is essential for this evaluation, but the scattering of the data at very low frequencies also puts certain experimental limitations on this requirement.

3. Results

The time–temperature superposed (TTS) linear viscoelastic master curve for the pure EP copolymer (with 84.3 wt% P) is shown in Fig. 2(a). This curve was developed from the data measured from 50 to 180 °C with the application of both vertical (b_T) and horizontal (a_T) shift factors with respect to a reference temperature $T_{ref}=100$ °C. The frequency shift factors (a_T) used for the construction of the master curve are plotted in Fig. 2(b) as a function of temperature. All data points were fitted by a straight line based on the Arrhenius relationship: $\log(a_T)=\Delta H_a/RT$, where the apparent activation energy ΔH_a was about 23 kJ mol^{-1}. The validity of the TTS principle over this wide temperature range suggests that the effects of any possible structural changes, such as lamellar formation or microphase separation, are of minor importance and, thus, are not further considered hereon.

In Fig. 2, the rheological response of the pure copolymer melt is typical of an entangled polymer with a crossover frequency close to 15 rad/s. In the case of the filled samples, the TTS rule does not hold due to dramatically terminal effects on the rheological spectra (as discussed below). Nevertheless, information regarding the effect of nanofillers on the polymer chain dynamics can be obtained by comparison of the rheological spectra of the filled samples with that of the unfilled sample measured at the same temperature. In Fig. 3(a) and (b) the dynamic moduli of the 10 and 20 wt% nanocomposites obtained at 50 and 180 °C, respectively, are plotted together with the dynamic moduli of the unfilled sample. It is apparent that at 50 °C (Fig. 3(a)), the crossover frequency at the terminal zone shifts to lower values with increasing filler concentration. Moreover, the storage moduli of

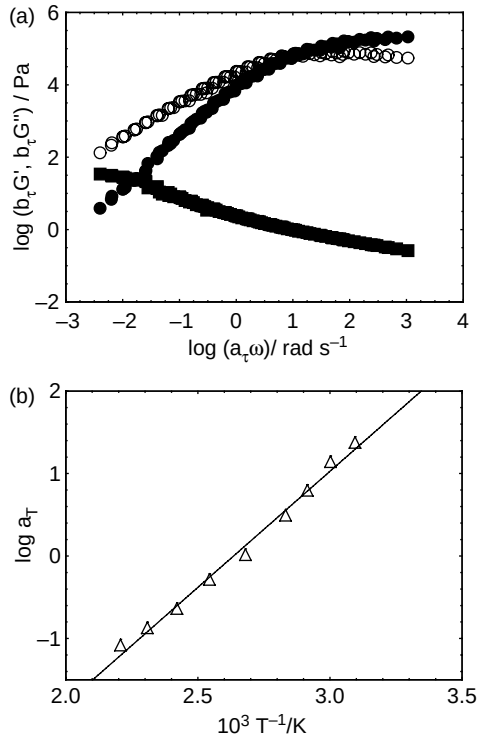

Fig. 2. (a) Time–temperature-superposed linear viscoelastic master curve for the pure EP copolymer (84.3 wt% P) at $T_{ref}=100$ °C. Filled circles: G', unfilled circles: G'' and filled squares: tan δ. (b) Temperature dependence of the shift factor, a_T (the solid line represents the linear fit based on the Arrhenius equation for activation energy).

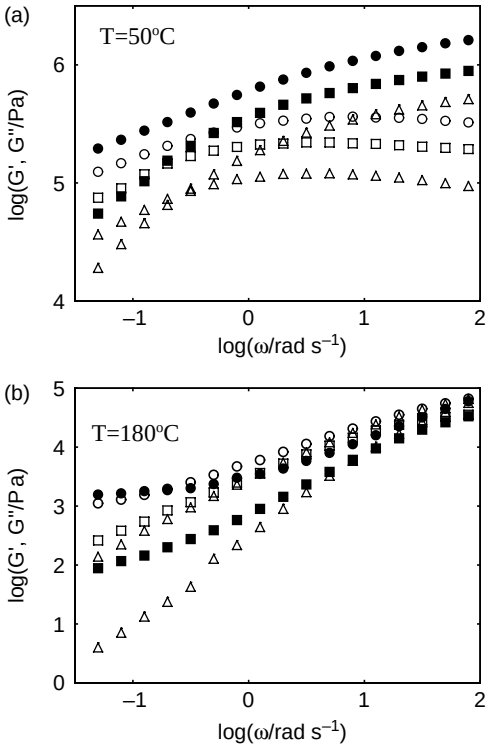

Fig. 3. Frequency dependence of storage and loss moduli for unfilled copolymer (triangles), 10 wt% (squares) and 20 wt% nanocomposites (circles). The filled symbol denotes G' and the unfilled symbol denotes G''. The data presented were collected at (a) $T=50$ °C and (b) $T=180$ °C.

the filled samples tend to a much higher plateau value (G_N^0) in comparison with the G_N^0 of the unfilled sample. This observation implies that the strong nanofiller-matrix interactions significantly affect the local dynamics of the polymer chains. At 180 °C (Fig. 3(b)), G_N^0 cannot be seen within the accessible rheological window. However, the strong MCNF–polymer interactions are manifested by the pronounced deviations in the low frequency region of the filled samples, which indicate the evolution of gelation.

In order to quantitatively study the evolution of gelation in MCMF-EP nanocomposites, the Winter–Chambon criterion was adopted to evaluate the curves of tan δ as a function of angular frequency for each MCNF nanocomposite at different temperatures. Fig. 4 illustrates the frequency dependence of tan δ for the 1 wt% MCNF nanocomposite at varying temperatures. For clarity, these curves have been shifted along the x-axis. At high temperatures (i.e. in the range 130–200 °C), the nanocomposite exhibited a pseudo-solid-like behavior; as determined from the positive slopes in the low frequency regime. Note that we favor the terminology 'pseudo-solid' rather than 'solid' behavior because the latter refers to a system that is: (i) frequency independent and (ii) G' significantly exceeds G''. In the present case, the first requirement is fulfilled only within the low frequency regime, whereas the second condition generally does not hold. At 129 °C, the nanocomposite reached the critical gel state; i.e. the tan $\delta(\omega)$ curve exhibited a zero-slope plateau in the low frequency regime. This behavior was further confirmed by observations at 128 and 125 °C, where the nanocomposite showed a liquid-like behavior, i.e. tan $\delta(\omega)$ curves exhibited negative slopes in the entire region of the rheological spectrum.

The values of storage and loss moduli for the 1 wt% nanocomposite at varying temperatures are illustrated in Fig. 5. It was seen that despite the nanocomposite at 200 °C is well within the pseudo-solid-like region (Fig. 4), G' was

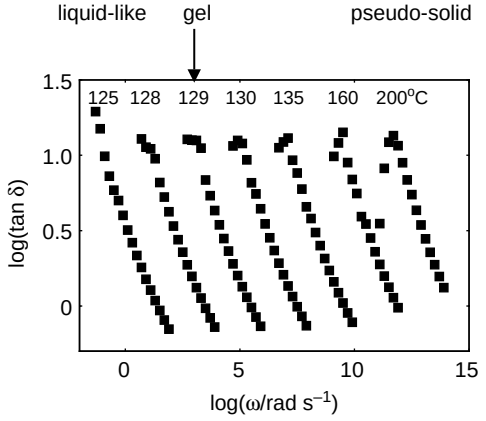

Fig. 4. Frequency dependence of tan δ for the 1 wt% nanocomposites at varying temperatures. The curves have been shifted along the x-axis. The gel point is indicated by the arrow.

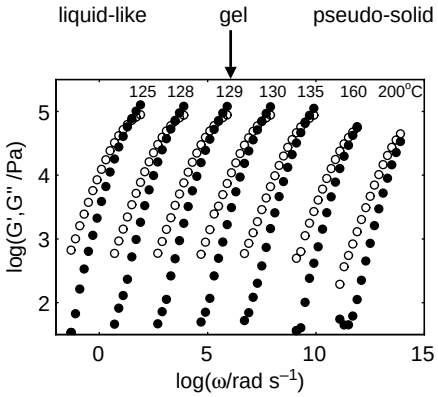

Fig. 5. Frequency dependence of storage (G', filled symbols) and loss modulus (G'', unfilled symbols) for the 1 wt% nanocomposites at varying temperatures during cooling. The curves have been shifted along the x-axis.

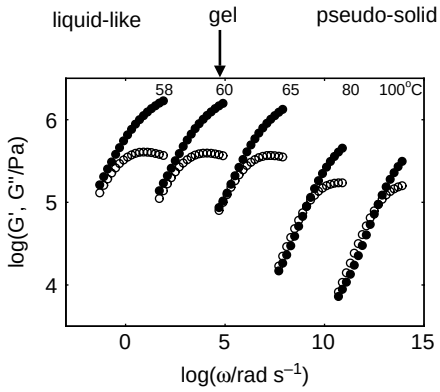

Fig. 7. Frequency dependence of storage (filled symbols) and loss modulus (unfilled symbols) for the 20 wt% nanocomposite at varying temperatures. The curves have been shifted along the x-axis.

consistently lower than the corresponding G'' in the entire frequency range considered. On the other hand, at lower temperatures, the crossover point of $G'(\omega)$ and $G''(\omega)$ curves falls within the accessible frequency range and their slopes approached the values expected for a typical melt (2 and 1, respectively). It is interesting to note that the data (not shown here) obtained upon heating was almost identical to that obtained upon cooling, indicating that the transition from pseudo-solid-like to liquid-like behavior was a thermo-reversible process.

Figs. 6 and 7 illustrate the frequency dependencies of tan δ, G' and G'' for the 20 wt% MCNF nanocomposite (the highest filler loading studied here) at varying temperatures. In tan $\delta(\omega)$ curves, the overall behavior of the 20 wt% nanocomposites was similar to that in the 1 wt% nanocomposite, i.e. the tan $\delta(\omega)$ curves exhibited pseudo-solid-like behavior at high temperatures (65, 80 and 100 °C) and liquid-like behavior at temperatures below 60 °C. The temperature for the occurrence of the critical gel state was about 60 °C in the 20 wt% nanocomposite, significantly lower than that in the 1 wt% nanocomposite (about 129 °C). For the 20 wt% nanocomposite at the gel point, G' was found to be larger than G'' in the entire frequency range studied; whereas for the 1 wt% nanocomposite, $G' > G''$ only occurred at high frequencies at the gel point. This behavior could be related to the temperature effect on the polymer matrix viscosity. As the gel point for the 20 wt% nanocomposite was only about 60 °C, the corresponding matrix viscosity was high, which led to a much higher G' than G'' in all frequency ranges.

Fig. 8 illustrates the tan $\delta(\omega)$ curves at the gel point for all the samples (with different concentrations of MCNF) studied. The critical gelation temperature, the relaxation exponent (n) and the stiffness of the critical gels (S) determined by Eqs. (2)–(4), are summarized in Figs. 9–11, respectively. With the increase in filler loading, the critical gelation temperature (T) was found to shift to a lower temperature and the gel became harder as could be seen from the lower relaxation exponent (n) and the higher stiffness of the gel (S). These figures could be divided into three regions: I, II and III, representing the filler loading less than 1 wt%, between 1 and 10 wt%, and larger than 10 wt%, respectively. Region I could be characterized by an abrupt negative slope in the $T(c)$ curve (Fig. 9), indicating that the curve approached an asymptotical value along the temperature axis at low c values (<0.5 wt%). At the same time, the $S(c)$ curve exhibited an abrupt increase while the $n(c)$ curve remained about unity. All these changes indicated

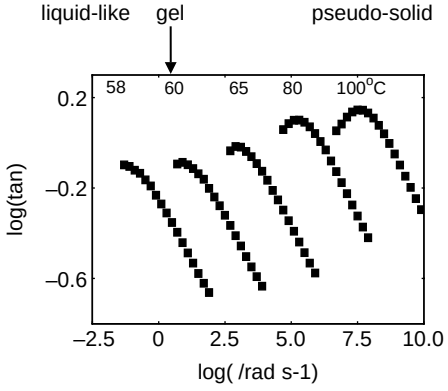

Fig. 6. Frequency dependence of tan δ for the 20 wt% nanocomposite at varying temperatures. The curves have been shifted along the x-axis. The gel point is indicated by the arrow.

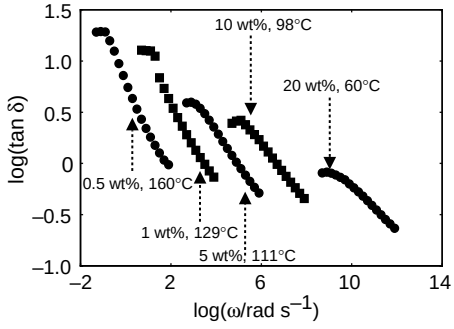

Fig. 8. Frequency dependence of tan δ of the nanocomposites at the gel point. Filler loading and temperatures are indicated. The curves have been shifted along the x-axis and the indicated temperatures have been approximated to the closest natural number.

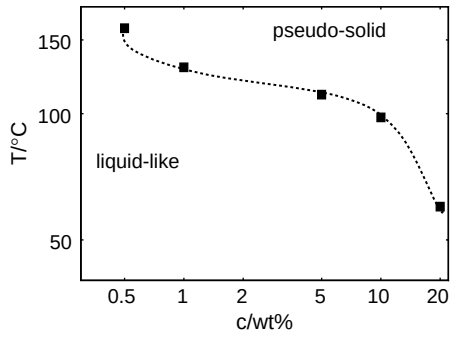

Fig. 9. Critical gelation temperature as a function of filler loading for MCNF-EP copolymer nanocomposites.

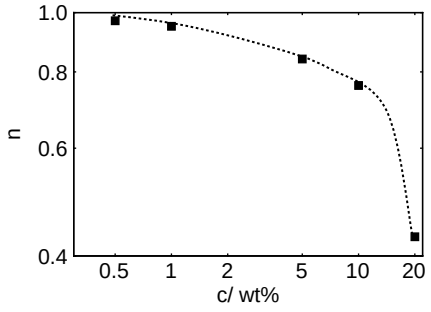

Fig. 10. Relaxation exponent (n) of critical gel as a function of filler loading for MCNF-EP copolymer nanocomposites.

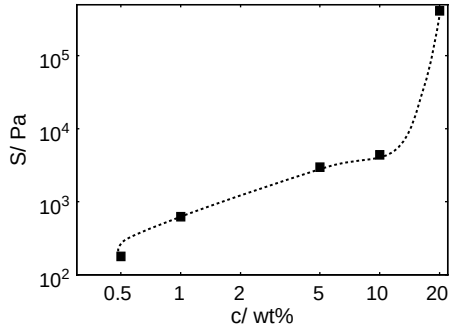

Fig. 11. Stiffness (S) of critical gel as a function of filler loading for MCNF-EP copolymer nanocomposites.

the existence of a percolation threshold for MCNF loading (<0.5 wt%), below which the physical gel could not be formed. Region II can be characterized by small negative slopes in both $T(c)$ and $n(c)$ curves, and a small positive slope in the $S(c)$ curve. The smooth changes in the rheological parameters of the critical gels within this region implied the strengthening of the physical gelation process. In region III, abrupt changes in all three plots, $T(c)$, $n(c)$ and $S(c)$, were again observed, indicating that the gelation mechanism in this region was different from that in region II.

Based on the SEM observation, no sign of MCNF aggregation was seen even in the 20 wt% nanocomposite (as shown in Fig. 1). If the aggregation of MCNFs indeed took place, the nanocomposite would exhibit opposite changes in the gel parameter (Figs. 9–11), because the aggregation of nanofibers would decrease the total surface area of MCNF in the polymer matrix, which would minimize the stability of the gel phase. However, this behavior was not seen in the 20 wt% nanocomposite (Fig. 9). We thus hypothesize that the difference in the gelation behavior between regions II and III was due to the change in polymer–filler and filler–filler interactions, which are discussed in detail next.

4. Discussion

4.1. Polymer chain dynamics and mechanism of gel formation

The dynamics of polymer-based nanocomposites are usually interpreted [29–33] with respect to the strengths of polymer–filler interactions and filler–filler interactions. These interactions are dependent on the nanofiller geometry, loading concentration and distribution, as well as the nature of the polymer matrix. In general, weak polymer–filler interactions promote phase segregation, whereas strong polymer–filler interactions promote the dispersion of nanoparticles [32]. Results from molecular dynamics simulations [33] of a system with repulsive or neutral polymer–filler interactions indicated that faster polymer dynamics, close to the nanofiller interface, could arise due to the decrease in the density of the polymer matrix. On the other hand, the densification of the polymer in the absorbed layer could slow down the polymer dynamics, close to attractive flat interfaces [34]. It has been proposed that the specific topography of a structured surface of the attractive fillers is critical for the reduced mobility of polymer segments along its surface. The overall dynamics is thus governed by the polymer segments being trapped within the surface energy wells and the polymer relaxation that occurs by migration of segments to neighboring wells. These effects can also explain the pronounced non-Gaussian character of monomer displacement of the absorbed polymer.

A gradual change of the polymer dynamics approaching the nanoparticle interface has been proposed [35] to rationalize the shift of the glass transition temperature (T_g) of the filled polymer melts (T_g can be increased or decreased in the case of attractive or non-attractive systems, respectively). This model, which considers several layers with different mobility, has also been employed to show that in repulsive systems, the polymer chains close to nanofillers tend to be elongated perpendicular to the interface; whereas in an attractive system, the absorbed polymer chains tend to be flattened along the nanofiller surface. It has been shown that, the polymer chains in the vicinity of the corners of fillers are subject to less pronounced restriction on their motion in comparison with the chains in the vicinity of the filler interface.

In the system considered here, the confined polymer chain dynamics induced by MCNFs could be assumed from the data plotted in Fig. 3(a), where all three samples considered (unfilled, 10 and 20 wt% nanocomposites) were within the liquid-like regime (Fig. 9). It could be seen that: (i) the terminal relaxation frequency decreased, and (ii) the plateau storage modulus G_N^0 increased with filler loading. The first observation

implied that the entangled polymer chains experience increased friction forces in the filled samples and, therefore, their motion is restricted and their relaxation is delayed. The second observation indicated that the inclusion of MCNFs increased the density of chain entanglements. This could be rationalized as follows: on the basis of the de Gennes scaling theory [36], G_N^0 scales with $1/M_e$ where M_e is the molecular weight between entanglements. Therefore, the increased G_N^0 observed in the filled samples implied lower M_e, which is equivalent to higher entanglement density. In other words, the strong interactions between MCNFs and copolymer chains have effectively increased the physical cross-linking density. These cross-link interactions induced by MCNFs are also responsible for the evolution of the gelation, which can be manifested at higher temperatures.

At elevated temperatures, the dispersion of MCNFs was more pronounced and the molten polymer chains could be strongly absorbed on the nanofiller surface. These well dispersed and polymer-swollen nanoparticles could produce 3D connectivity that was the origin of the pseudo-solid-like response in rheology. At the percolation point, the MCNFs did not necessarily have to be in direct contact with each other, given that the polymer matrix could swell the nanofillers and, hence, increase their apparent volume fraction. The polymer segments could be in contact, though not tightly bound, with the nanoparticles and form a dense layer in the interface between the adjacent nanofillers. The adsorption of the polymer chains on the nanoparticles would result in a significant decrease of the free energy; meanwhile the polymer entropy was also reduced due to the localization of polymer segments to form the higher density interfacial shells [37]. It is our opinion that the thermodynamic driving forces, such as polymer–polymer, polymer–MCNF and MCNF–MCNF interactions, are significantly altered upon cooling, which could lead to a gradual loss of the pseudo-solid-like behavior in the nanocomposite melt. In addition, as the viscosity of the polymer matrix also increases during cooling, the more viscous rheological behavior of the nanocomposite melt would further hinder the diffusion of polymer chains. The combined effect might completely eliminate the gelation behavior at lower temperatures.

As MCNFs approach each other, the polymer chains are able to interact with two (or more) nanoparticles at the same time. The localization of the polymer segments to these positions is energetically favored [37], despite the fact that the overall entropy of the polymer matrix is unfavorable. The segments of the adsorbed chains can be placed in the interface shells, but can also adopt loop (non interface units with two ends in contact with the same particle) and bridge (non interface units with two ends in contact with two different particles) conformations [38]. Obviously, the concept of the bridge conformation of the polymer segments is valid in nanocomposites with filler loading surpassing a minimum value. Occupation of these highly energetic favorable bridge positions at high enough filler loading would alter the rheological response in region III, as manifested by the abrupt change in the slopes of $T(c)$, $n(c)$ and $S(c)$ curves observed in Figs. 9–11, respectively. In other words, the bridge conformation of the polymer chains in the concentrated nanocomposites considerably enhances the 3D connectivity of the system, an effect that is reflected in the broader range of thermal stability (Fig. 9), lower relaxation exponent n (Fig. 10) and higher stiffness S (Fig. 11) of the gel phase. Therefore, the bridge formation of the polymer segments at filler loading above 10 wt% modifies the mechanism of physical gelation, in comparison with that in the low c region (e.g. region II).

4.2. Percolation threshold

The estimated percolation threshold (<0.5 wt%) in the present system, determined by the rheological method, is directly related to the high aspect ratio of the nanofibers (MCNFs). The percolation threshold for overlapping prolates in the case of well dispersed needle-like particles has been estimated [39], in which the threshold value is proportional to the inverse of the aspect ratio and has a value ranging from 0.0006 to 0.002 (in volume ratio) for the aspect ratio between 250 and 1000 (similar to that of the MCNF). The percolation threshold is closely related to but cannot be totally defined from the geometry of the dispersed particles, because it also depends upon the relative strength of polymer–polymer, filler–filler and polymer–filler interactions. The nanoparticle geometry, the type of polymer matrix, the preparation scheme of nanocomposites and the experimental method used to evaluate the percolation point are all known to affect the determination of the percolation threshold. For CNTs nanocomposites, the percolation threshold has been reported in the range of 10^{-3}–1 wt% [40–44]. The extent of the polymer induced swelling of fillers depends on the nature of the polymer matrix. For example, the percolation threshold of carbon black aggregates has been correlated with the polymer matrix surface tension [45]. In the case of thermoplastic matrix, a relatively high percolation threshold is expected due to the high viscosity of the polymer, which hinders the dispersion of nanofillers.

In the literature, varying procedures to control the nanocomposite morphology and, therefore, to lower the percolation threshold has been proposed. For example, the close packing of polyvinyl acetate (PVAc) particles obtained during evaporation of the aqueous emulsion of single-walled carbon nanotube (SWNT)-PVAc precomposite has been employed for the localization of SWNT in such a way that a 3D network with remarkably low percolation threshold could be produced [43]. In another study, polymerization of the viscous poly(butylene terephthalate) matrix in the presence of CNTs has been used to achieve a higher level of CNTs dispersion and, therefore, enhance the formation of the gel phase [44]. It has been shown experimentally that percolation takes place at lower filler loadings by substitution of entangled carbon nanotubes from aligned ones [40]. Computational analysis indicates that van der Waals interactions between nanotubes result in their mutual local alignment and increase the percolation threshold [46].

It is instructive to note that the percolation threshold is also sensitive to the experimental methods chosen. For example, the connectivity percolation determined by the electrical

conductivity (σ) method usually precedes the percolation of rigidity defined by rheology [47]. However, measurements of electrical conductivity (σ) over a wide range of nanotube loading (c) and extrapolation of $\sigma(c)$ curve to the pure nanotube film leads to a significantly lower value than that expected [48]. The presence of a polymer shell around the nanofillers can reduce the interfiller electrical connectivity and, thus, increase the connectivity percolation determined by σ (in the case of non- or semi-conducting polymers), but at the same time can increase the apparent molar volume of the nanofillers and thus decrease the percolation of rigidity defined by rheology.

In this study, the percolation threshold was determined by the Winter–Chambon criterion. It is necessary to point out that there are other criteria that can also be used to characterize the state of gelation. For example, it has been reported [49] that the development of a critical strain can be used to monitor the structural changes during chemical cross-linking of an epoxy-based composite. This criterion, although being sensitive to the viscoelasicity of the bulk phase and able to probe the evolution of physical gelation upon increasing nanofiller loading at a constant temperature, cannot probe the evolution of pseudo-solid-like response upon heating for a given composite. The shift of the G'/G'' crossover point along the frequency axis has also been demonstrated as another criterion to determine the phase transitions in polymers [50,51]. From the data presented above, the application of the G'/G'' crossover criterion can indeed detect the evolution of the physical gels in a qualitative manner. For example, in Fig. 3, a well defined crossover point is observed for the 20 wt% nanocomposite at 180 °C, but not at 50 °C, indicating a temperature induced transition. However, this criterion does not offer sufficient sensitivity as the Winter–Chambon criterion, with which the pseudo-solid-like response for the 20 wt% nanocomposite was found to be at 60 °C (the crossover point within the accessible rheological window was only observed at much higher temperatures). Therefore, it is evident that the Winter–Chambon criterion, based on the more sensitive parameter tan δ (rather than G' and G''), provides a more accurate estimate of the percolation threshold and the gelation point.

Apart from the factors mentioned above, a clear conclusion of this study is that the temperature is also a critical parameter affecting the rigidity percolation point in nanocomposites. For a given nanocomposite, the effect of temperature is so pronounced that the percolation of rigidity seems to be a delicate balance between the nanofiller loading and temperature (Fig. 9). In particular, moving across the concentration axis of Fig. 9, it is clear that the adsorption of the polymer to the nanofiller interface and, therefore, the apparent volume fraction of the swollen nanoparticles are greatly influenced by temperature. A nanocomposite with a given filler concentration can be viewed as a percolated system having a critical temperature, above of which the 3D connectivity of the polymer swollen nanoparticles is detected. Moving across the temperature axis of Fig. 9, it is obvious that the percolation temperature dropped with the filler concentration, resulting in a wider region of thermodynamic stability of the gel phase at high c values. Finally, it is of interest to note that the dependence of the percolation temperature as a function of nanofiller loading (c) can indicate the internal structural changes in the melt, e.g. the bridging conformation of polymer segments at concentrated samples.

5. Conclusions

The MCNF-reinforced elastomeric EP copolymer nanocomposite melts exhibited pronounced deviations from the ideal melt behavior in the low frequency regime. The unique rheological behavior suggests the formation of a 3D percolated network at high temperatures. The physical gelation induced by MCNFs is a thermo-reversible process and its origin can be attributed to the interactions of polymer swollen carbon nanofibers. These strong MCNF–polymer interactions are also present at relatively low temperatures and result in an increased entanglement density of the polymer chains. However, the temperature is a critical parameter affecting the rigidity percolation point of nanocomposites, where a delicate balance exists between the nanofiller loading and the percolation temperature.

Abrupt changes in the critical gelation temperature (T), the stiffness of the gel (S) and the relaxation exponent (n) were observed above 10 wt% MCNF loading. This behavior is consistent with the bridge conformation of polymer segments (i.e. non-interface units with two ends in contact with two different nanofillers) at high filler loading. This bridge conformation of the polymer chains considerably enhances the 3D connectivity of the system at high c region, an effect that is reflected in the broader range of thermodynamic stability, the lower relaxation exponent n and the higher stiffness S of the gel. Occupation of these highly energetic favorable bridge positions not only modifies the behavior of the rheological response of the nanocomposite, but also alters the gelation mechanism in the high c region, in comparison with the low c-region.

Acknowledgements

The financial support of this work was provided by the Office of Naval Research (N000140310932) and the National Science Foundation (DMR-0405432). The authors acknowledge the assistance of Dr Mikhail Gelfer for the rheological experiment.

References

[1] Baughman RH, Zakhidov AA, de Heer WA. Science 2002;297:787.
[2] Hammel E, Tang X, Trampert M, Schmitt T, Mauthner K, Eder A, et al. Carbon 2004;42:1153.
[3] Qian D, Dickey EC, Andrews R, Rantell T. Appl Phys Lett 2000;76:2868.
[4] Schadler LS, Giannaris SC, Ajayan PM. Appl Phys Lett 1998;73:3842.
[5] Coleman JN, Cadek M, Blake R, Nicolosi V, Ryan KP, Belton C, et al. Adv Funct Mater 2004;14:791.
[6] Biercuk MJ, Llaguno MC, Radosavljevic M, Hyun JK, Johnson AT, Fischer JE. Appl Phys Lett 2002;80:2767.
[7] Hirsch A. Angew Chem Int Ed 2002;41:1853.
[8] Sun Y-P, Fu K, Lin Y, Huang W. Acc Chem Res 2002;35:1096.

[9] Niyogi S, Hamon MA, Hu H, Zhao B, Bhowmik P, Sen R, et al. Acc Chem Res 2002;35:1105.
[10] Blake R, Gunko YK, Coleman J, Cadek M, Fonseca A, Nagy JB, et al. Am Chem Soc 2004;126:10226.
[11] Datta S, Srinivas S, Cheng CY, Tsou A, Lohse DJ. Rubber World 2003; 229:55.
[12] Horst RH, Winter HH. Macromolecules 2000;33:130.
[13] Pogodina NV, Lavrenko VP, Srinivas S, Winter HH. Polymer 2001;42: 9031.
[14] Yurekli K, Krishnamoorti R, Tse MF, Mcelrath KO, Tsou AH, Wang HC. J Polym Sci, Part B: Polym Phys 2001;39:256.
[15] Mitchell CA, Bahr JL, Arepalli S, Tour JM, Krishnamoorti R. Macromolecules 2002;35:8825.
[16] Potschke P, Fornes TD, Paul DR. Polymer 2002;43:3247.
[17] Liu C, Zhang J, He J, Hu G. Polymer 2003;44:7529.
[18] Kharchenko SB, Douglas JF, Obrzut J, Grulke EA, Migler KB. Nat Mater 2004;3:564.
[19] Krishnamoorti R, Yurekli K. Curr Opin Colloid Interface Sci 2001;6:464.
[20] Krishnamoorti R, Giannelis EP. Macromolecules 1997;30:4097.
[21] Hough LA, Islam MF, Janmey PA, Yodth AG. Phys Rev Lett 2004;93: 168102.
[22] Rodriguez NM. J Mater Res 1993;8:3233.
[23] Toki S, Sics I, Liu LZ, Hsiao BS, Tsou AH, Datta S. Am Chem Soc Rubber Div Prepr 2003;2055.
[24] Kelarakis A, Yoon K, Sics I, Somani R, Hsiao BS, Chu B. Polymer 2005; 46:5103.
[25] Lim J, Yun W, Yoon M, Lee SK, Kim C, Kim K, et al. Synth Mater 2003; 139:521.
[26] Oh SJ, Jung JC, Zin W-C. J Colloid Interface Sci 2001;238:43.
[27] Chambon F, Winter HH. J Rheol 1987;31:683.
[28] Winter HH, Chambon F. J Rheol 1986;30:367.
[29] Leonov AI. J Rheol 1990;34:1039.
[30] Fu BX, Gelfer MY, Hsiao BS, Philips S, Viers B, Blanski R, et al. Polymer 2003;44:1499.
[31] Chabert E, Bornert M, Bourgeat-Lami E, Cavaille J-Y, Dendievel R, Gauthier C, et al. Mater Sci Eng A 2004;381:320.
[32] Smith JS, Bedrov D, Smith GD. Compos Sci Technol 2003;63:1599.
[33] Smith SD, Bedrov D, Li L, Byutner O. J Chem Phys 2002;117:9478.
[34] Smith GD, Bedrov D, Borodin O. Phys Rev Lett 2003;90:226103.
[35] Starr WF, Schroder TB, Glotzer SC. Phys Rev E 2001;64:021802.
[36] de Gennes PG. J Chem Phys 1971;55:572.
[37] Bedrov D, Smith GD, Smith JS. J Chem Phys 2003;119:10438.
[38] Vacatello M. Macromol Theory Simul 2003;12:86.
[39] Garboczi EJ, Snyder KA, Douglas JF, Thorpe MF. Phys Rev E 1995; 52:819.
[40] Sandler JKW, Kirk JE, Kinloch IA, Shaffer MSP, Windle AH. Polymer 2003;44:5893.
[41] Barrau S, Bemont P, Peigney A, Laurent C, Lacabanne C. Macromolecules 2003;36:5187.
[42] Stephan C, Nguyen TP, Lahr B, Blau W, Lefrant S, Chauvet O. J Mater Res 2002;17:396.
[43] Grunlan JC, Mehrabi AR, Bannon MV, Bahr JL. Adv Mater 2004;16:150.
[44] Nogales A, Broza G, Roslaniec Z, Schulte K, Sics I, Hsiao BS, et al. Macromolecules 2004;37:7669.
[45] Miyasaka K, Watanabe K, Jojima E, Aida H, Sumita M, Ishikawa K. J Mater Sci 1982;17:1610.
[46] Grujicic M, Cao G, Roy WN. J Mater Sci 2004;39:4441.
[47] Head DA, Levine AJ, MacKinosh FC. Phys Rev E 2003;68:061907.
[48] Kilbride BE, Coleman JN, Fraysse J, Fournet P, Cadek M, Drury A, et al. J Appl Phys 2002;92:4024.
[49] Chiou B-S, Raghavan SR, Khan SA. Macromolecules 2001;34:4526.
[50] Kelarakis A, Mingvanish W, Daniel C, Li H, Havredaki V, Booth C, et al. Phys Chem Chem Phys 2000;2:2755.
[51] Kelarakis A, Havredaki V, Booth C. Macromol Chem Phys 2005;205: 1594.